Space Saving and Power Efficient Readout System for Cosmic-Ray Muon Radiography

Tomohisa Uchida*, Member, IEEE*, Hiroyuki K. M. Tanaka, and Manobu Tanaka*, Member, IEEE*

***Abstract*—Cosmic-ray muon radiography has been used to probe the internal structure of volcanoes. To overcome limitations on constructing an observation station, we developed a small-sized readout system with power consumption low enough to be powered by a small solar-power system. The system can be placed near a volcano and can detect cosmic-ray muons that penetrate the volcano and subsequently generate an angular distribution of the muons. The system can be connected to a PC placed remotely from the station, using a wired or wireless network. The PC can show the angular distribution of the muons on a web browser. We used this system to monitor an actual volcano. The obtained clear image of the volcano indicates that the performance of the readout system is sufficient for cosmic-ray muon radiography.**

***Index Terms*—Data acquisition systems, FPGAs, muon detectors.**

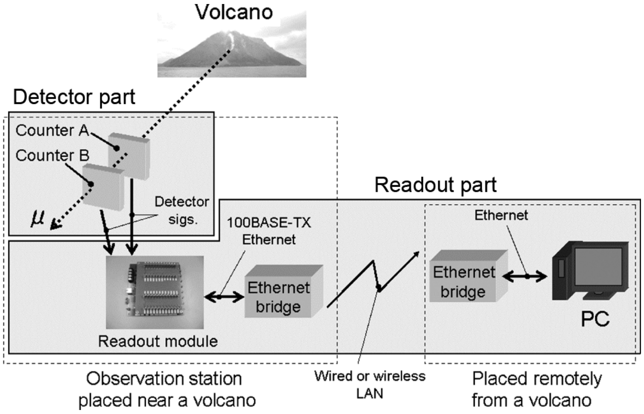

Fig. 1. Detection system for cosmic-ray muon radiography.

I. INTRODUCTION

ALTHOUGH cosmic-ray muon radiography has been applied to interrogation of cargo containers [1], [2] and Egyptian pyramids [3], it was first applied to volcanoes, to predict volcanic eruptions, in 1996 [4]. Cosmic-ray muons with small horizontal angles at sea level have high energy, which can penetrate through a volcano. The amount of energy lost by muons while passing through matter is dependent on the density of that matter. The angular distribution of muons can then be used to calculate the density profile of a volcano and, hence, its internal structure. Therefore, a cosmic-ray muon radiography detection system is needed to determine the paths of these muons and to count the events. Early detection systems were based on position-sensitive plastic scintillation counters, with readout systems based on Nuclear Instrumentation Modules (NIMs) and Computer Automated Measurement And Control (CAMAC) modules [4]–[7]. Since their power consumption is large, a commercial power supply is required. It is therefore difficult to place an observation station near a volcano because commercial power sources are not always available and access to the system is limited. This limits the location of observation stations.

To overcome this limitation, an "emulsion imaging system" using nuclear emulsion films has been developed [8]. This system overcomes the limitations on constructing observation stations because it is small and has no requirement for a power source. As a result, muon-detection systems can be placed near targets, pointing toward a topographically prominent feature of interest, e.g., the vent or crater of a volcano. While cosmic-ray muon radiography could therefore reveal the internal structure of a volcano [9], [10], these observations are not in real-time. We therefore could not determine changes over time. Real time readings, however, may help in predicting eruptions. Electronics are required for real-time observation. One solution is to employ a small solar-powered system and a wireless Local Area Network (LAN). To create such a system, a space and power effective readout system is required. To meet these requirements, we have developed a readout system powered by a small solar-powered system.

II. DETECTION SYSTEM

The detection system detects cosmic-ray muons penetrating through a volcano, determines their paths, and generates their angular distribution as a histogram.

A block diagram of the detection system is shown in Fig. 1. The system consists of two major parts: a detector and a readout instrument. The detector detects the cosmic-ray muons using two position-sensitive counters. The readout instrument processes signals from the counters and generates a histogram of angular distribution.

The detector is placed near a volcano, less than 1 km from its surface. This short distance makes contributions from soft components—electrons, positrons, and photons—negligible, because most soft components arise from decay of the muons.

Manuscript received November 12, 2008; revised January 27, 2009. Current version published April 08, 2009.

T. Uchida is with the Department of Physics, University of Tokyo, Bunkyo-ku, Tokyo 113-0033, Japan (e-mail: uchida@hep.phys.s.u-tokyo.ac.jp).

H. K. M. Tanaka is with the Earthquake Research Institute, University of Tokyo, Bunkyo-ku, Tokyo 113-0032, Japan.

M. Tanaka is with the IPNS, High Energy Accelerator Research Organization (KEK), Tsukuba 305-0801, Japan.

Color versions of one or more of the figures in this paper are available online at http://ieeexplore.ieee.org.

Digital Object Identifier 10.1109/TNS.2009.2014866

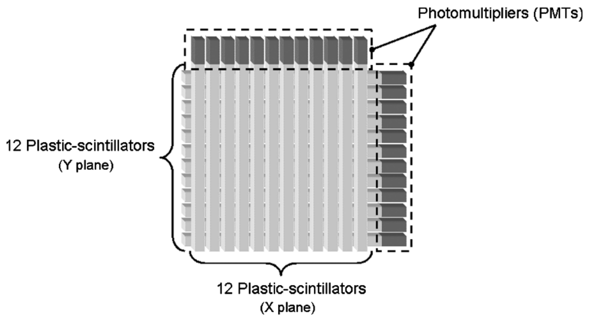

Fig. 2. Schematics of the counter.

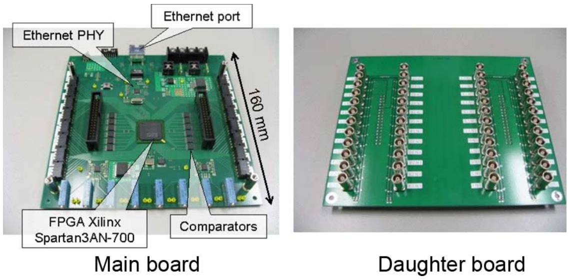

Main board Daughter board

Fig. 3. Photographs of the main and daughter boards.

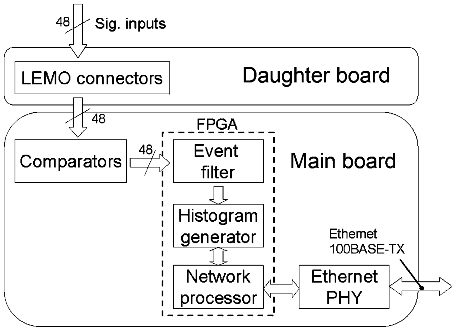

Fig. 4. Block diagram of the readout module.

If their contribution is not negligible, an iron plate is inserted between the counters to generate a cascade shower by the soft components [6], [7]. Since each event of the shower gives rise to multiple hits on the counter, the event can be removed by readout electronics.

Fig. 2 shows a schematic of the counter, which consists of two plates of plastic-scintillator arrays. The X- and Y-planes detect the horizontal and vertical positions of a muon, respectively. Each plane consists of 12 scintillators, $15 \times 70 \times 1000\ \mathrm{mm}$ in size, with each counter having $144 = 12 \times 12$ total pixels. A Mamamatsu R7724 photomultiplier tube (PMT), adapted to low power consumption using a high-resistance voltage divider, is mounted onto each scintillator. The total number of anode signals from PMTs of two counters is 48. High voltage power for all PMTs is supplied by a single Matsusada Precision Inc. HAR-2N150 power source, with the measured power consumption of this high voltage system, including PMTs, of about 40 W, 100VAC.

All signals of the PMTs are processed by the readout system, generating a histogram of the angular distribution of the muons. The readout system consists of a readout module, Ethernet bridges, and a PC placed remotely from the observation station. The readout module processes signals from the detector, generates a histogram as a web page, and works as a web server. The detector and readout systems are connected through a wired or wireless network by the Ethernet bridges. The histogram can be obtained from the PC using a web browser. This module plays a central role in this system, and its details are described in the next section. In addition, all the devices, with the exception of the readout module, are commercial products. Thus, a cost-effective, high performance system can be easily constructed.

The main issue concerning the development of this system is low power consumption, which is required for a small solar powered system. The total power budget is about 60 W. The maximum solar module that can be employed for the observing station is about $4\ \mathrm{m}^2$. Since the rated power of a standard solar module of area $1\ \mathrm{m}^2$ is around 160 W, the power supply capability is about 600 W. Taking the sunshine ratio into consideration, the effective average power is about 60 W. The measured power consumption of the high voltage system including PMTs is about 40 W, 100VAC. One of the candidates for the wireless bridge is Allied Telesis Co. AT-TQ4551, with a communication distance of up to 22 km. The maximum power consumption of this bridge is about 10 W, 100 VAC. Therefore, the power consumption required by the readout module is less than 10 W.

III. READOUT MODULE

The readout module is $35 \times 160 \times 160\ \mathrm{mm}$ in size and 420 g in weight and consists of a main and a daughter board. (Fig. 3). The daughter board is a connector changer, so that various types of connectors can be used, and is mounted onto the main board. The signals from the PMTs are processed by the main board. The main parts are the comparators, a Field-Programmable Gate Arrays (FPGA, Xilinx Spartan3AN-700) [11], and an Ethernet physical-layer device (PHY, SMSC LAN8700i) [12].

Fig. 4 shows a block diagram of the readout module, which consists of LEMO connectors, comparators, an event filter, a histogram generator, a network processor, and an Ethernet PHY. To reduce power consumption, the frequency of the system clock for the FPGA is low, 50-MHz. The event filter, the histogram generator, and the network processor are implemented on the single FPGA.

The detector signals are received and digitized by the comparators. The event filter selects events that can be used to construct muon paths and generates "information data" for the paths. The information data consists of detection times and positions of the two counters. A histogram of the angular distribution of the selected events is generated by the histogram generator from the path information. The network processor deals with subsequent network protocols to access the histogram from a remote PC using a web browser. The network protocols used for this purpose are Ethernet, Internet Protocol (IP), Transmission Control Protocol (TCP), Hyper Text Transfer Protocol (HTTP), and Hyper Text Markup Language (HTML). The Ethernet PHY converts signals between the FPGA and Ethernet. The details of the circuits on the FPGA are described in the following sections.

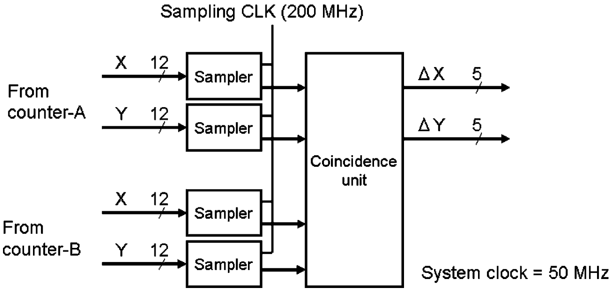

Fig. 5. Block diagram of the event filter.

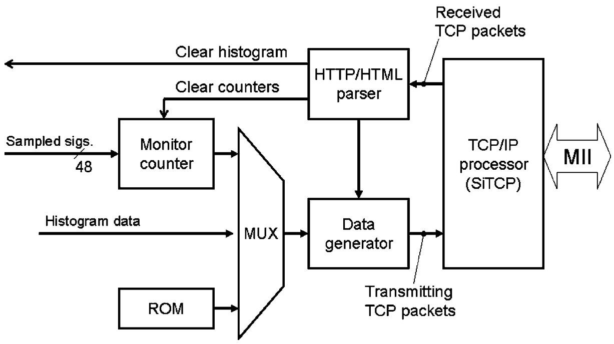

Fig. 6. Block diagram of the network processor.

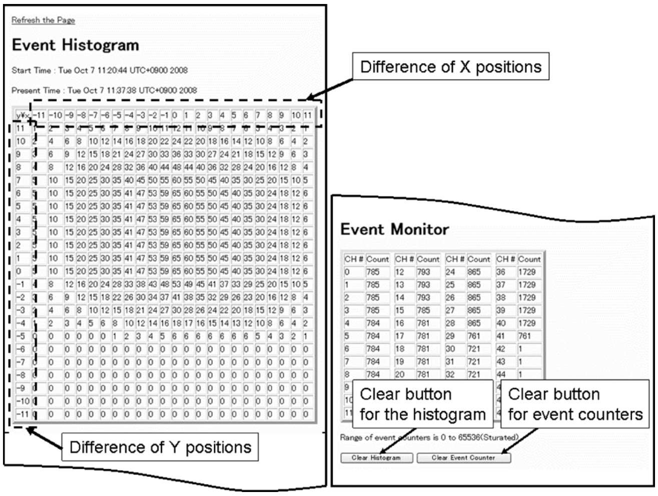

Event Histogram

Start Time : Tue Oct 7 11:20:44 UTC+0900 2008

Present Time : Tue Oct 7 11:37:38 UTC+0900 2008

y¥x	−11	−10	−9	−8	−7	−6	−5	−4	−3	−2	−1	0	1	2	3	4	5	6	7	8	9	10	11
11	1	2	3	4	5	6	7	8	9	10	11	12	11	10	9	8	7	6	5	4	3	2	1
10	2	4	6	8	10	12	14	16	18	20	22	24	22	20	18	16	14	12	10	8	6	4	2
9	3	6	9	12	15	18	21	24	27	30	33	36	33	30	27	24	21	18	15	12	9	6	3
8	4	8	12	16	20	24	28	32	36	40	44	48	44	40	36	32	28	24	20	16	12	8	4
7	5	10	15	20	25	30	35	40	45	50	55	60	55	50	45	40	35	30	25	20	15	10	5
6	5	10	15	20	25	30	35	41	47	53	59	65	60	55	50	45	40	35	30	24	18	12	6
5	5	10	15	20	25	30	35	41	47	53	59	65	60	55	50	45	40	35	30	24	18	12	6
4	5	10	15	20	25	30	35	41	47	53	59	65	60	55	50	45	40	35	30	24	18	12	6
3	5	10	15	20	25	30	35	41	47	53	59	65	60	55	50	45	40	35	30	24	18	12	6
2	5	10	15	20	25	30	35	41	47	53	59	65	60	55	50	45	40	35	30	24	18	12	6
1	5	10	15	20	25	30	35	41	47	53	59	65	60	55	50	45	40	35	30	24	18	12	6
0	5	10	15	20	25	30	35	41	47	53	59	65	60	55	50	45	40	35	30	24	18	12	6
−1	4	8	12	16	20	24	28	33	38	43	48	53	49	45	41	37	33	29	25	20	15	10	5
−2	3	6	9	12	15	18	22	26	30	34	37	41	38	35	32	29	26	23	20	16	12	8	4
−3	2	4	6	8	10	12	15	18	21	24	27	30	28	26	24	22	20	18	15	12	9	6	3
−4	1	2	3	4	5	6	8	10	12	14	16	18	17	16	15	14	13	12	10	8	6	4	2
−5	0	0	0	0	0	0	1	2	3	4	5	6	6	6	6	6	6	6	5	4	3	2	1
−6	0	0	0	0	0	0	0	0	0	0	0	0	0	0	0	0	0	0	0	0	0	0	0
−7	0	0	0	0	0	0	0	0	0	0	0	0	0	0	0	0	0	0	0	0	0	0	0
−8	0	0	0	0	0	0	0	0	0	0	0	0	0	0	0	0	0	0	0	0	0	0	0
−9	0	0	0	0	0	0	0	0	0	0	0	0	0	0	0	0	0	0	0	0	0	0	0
−10	0	0	0	0	0	0	0	0	0	0	0	0	0	0	0	0	0	0	0	0	0	0	0
−11	0	0	0	0	0	0	0	0	0	0	0	0	0	0	0	0	0	0	0	0	0	0	0

Event Monitor

CH #	Count	CH #	Count	CH #	Count	CH #	Count
0	785	12	793	24	865	36	1729
1	785	13	793	25	865	37	1729
2	785	14	793	26	865	38	1729
3	785	15	785	27	865	39	1729
4	784	16	781	28	865	40	1729
5	784	17	781	29	761	41	761
6	784	18	781	30	721	42	1
7	784	19	781	31	721	43	1
8	784	20	781	32	721	44	1
9							
10							
11							

Range of event counters is 0 to 65536(Sturated)

Fig. 7. Web page showing the histogram.

A. Event Filter

The event filter selects events that can be used to construct the muon paths and generates path information. Noise signals and multiple-hit events generated by soft components are excluded by this circuit.

Fig. 5 shows a block diagram of the event filter, which consists of samplers and a coincidence unit. To reduce sampling errors, input signals from the comparators are sampled at 200 MHz (5-ns period). The sampled signal is stretched to 40 ns when the pulse width is shorter than 40 ns to synchronize with the system clock. The coincidence unit selects events from the sampled signals and generates their path information. Because one signal arises from each scintillator-array plane, the two signals from the same counter are detected simultaneously, and all signals must be within a coincidence window. The window size can be set from 0 to 2 μs by a 20 ns unit. The path information consists of two 5-bit-width detectors of position differences between the positions of the two counters in both the horizontal, ΔX, and vertical, ΔY, planes.

B. Histogram Generator

The histogram is generated in a 32 bit-width internal memory of the FPGA. The path information generated by the coincidence unit is used as the 10 bit-width address for access to the internal memory. Data corresponding to the address are counted when an event is detected. These data are read by the network processor, described in the next section, when a remote PC accesses this histogram.

C. Network Processor

The network processor deals with network protocols to access the histogram from a remote PC using a web browser. The PC can execute instructions, including obtaining and clearing histogram data. In addition, this block has event counters for monitoring the detectors. Their data are also obtained and cleared using a web browser.

The network protocols are processed by a hardware circuit specialized for a web page. There is no CPU and no other programmable sequencers in this block. This design has advantages in power consumption and failure rate while running.

Fig. 6 shows a block diagram of the network processor, which consists of a TCP/IP processor (SiTCP) [13], [14], a HTTP/HTML parser, event counters, a read only memory (ROM), a multiplexer (MUX), and a data generator. This module works as a web server. The network protocols processed by this block are HTML, HTTP, TCP, IP, and Ethernet. The SiTCP processes TCP, IP, and Ethernet. The SiTCP is a hardware based TCP/IP processor, which can be implemented on a FPGA with no other external devices, e.g., memory devices [13], [14]. The parser analyzes HTML and HTTP data extracted from TCP packets by the SiTCP and executes commands from the remote PC. There are three commands: "clear histogram data," "clear event counters," and "obtain histogram data". There are clear buttons for the histogram data and event counters on a web page (Fig. 7). A command packet to clear histogram data or event counters is transmitted from the PC when the clear button is clicked. Acknowledge packets for the commands are sent by this block when the histogram data or the event counters are cleared. To measure the counting rate of the detectors, the event counters total the detector signals for one second after the clear command is received.

Fig. 8 shows a HTML source file of the web page, which consist of three parts: fixed data, histogram data, and values of event counters. The fixed data are a HTML header, HTML codes, and Java scripts. The Java scripts are used to reduce loads on this block. The fixed data are read from the ROM. The histogram data and event counter values are read from the histogram memory and event counters, respectively. These data sources are selected by the data generator with the MUX when data for the web page are generated. The SiTCP transmits these

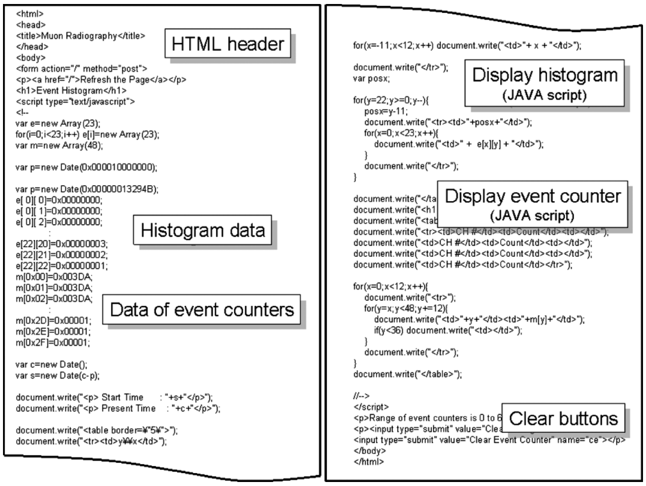

```
<html>
<head>
<title>Muon Radiography</title>
</head>
<body>
<form action="/" method="post">
<p><a href="/">Refresh the Page</a></p>
<h1>Event Histogram</h1>
<script type="text/javascript">
<!--
var e=new Array(23);
for(i=0;i<23;i++) e[i]=new Array(23);
var m=new Array(48);

var p=new Date(0x000010000000);

var p=new Date(0x00000013294B);
e[ 0][ 0]=0x00000000;
e[ 0][ 1]=0x00000000;
e[ 0][ 2]=0x00000000;
             :
e[22][20]=0x00000003;
e[22][21]=0x00000002;
e[22][22]=0x00000001;
m[0x00]=0x003DA;
m[0x01]=0x003DA;
m[0x02]=0x003DA;
             :
m[0x2D]=0x00001;
m[0x2E]=0x00001;
m[0x2F]=0x00001;

var c=new Date();
var s=new Date(c-p);

document.write("<p> Start Time      : "+s+"</p>");
document.write("<p> Present Time    : "+c+"</p>");

document.write("<table border=¥"5¥">");
document.write("<tr><td>y¥¥x</td>");
```

```
for(x=-11;x<12;x++) document.write("<td>"+ x + "</td>");

document.write("</tr>");
var posx;

for(y=22;y>=0;y--){
    posx=y-11;
    document.write("<tr><td>"+posx+"</td>");
    for(x=0;x<23;x++){
        document.write("<td>" +  e[x][y] + "</td>");
    }
    document.write("</tr>");
}

document.write("</ta
document.write("<h1
document.write("<tab
document.write("<tr><td>CH #</td><td>Count</td><td></td>");
document.write("<td>CH #</td><td>Count</td><td></td>");
document.write("<td>CH #</td><td>Count</td><td></td>");
document.write("<td>CH #</td><td>Count</td></tr>");

for(x=0;x<12;x++){
    document.write("<tr>");
    for(y=x;y<48;y+=12){
        document.write("<td>"+y+"</td><td>"+m[y]+"</td>");
        if(y<36) document.write("<td></td>");
    }
    document.write("</tr>");
}
document.write("</table>");

//-->
</script>
<p>Range of event counters is 0 to 6
<p><input type="submit" value="Clea
<input type="submit" value="Clear Event Counter" name="ce"></p>
</body>
</html>
```

Fig. 8. HTML source for a web page showing the histogram.

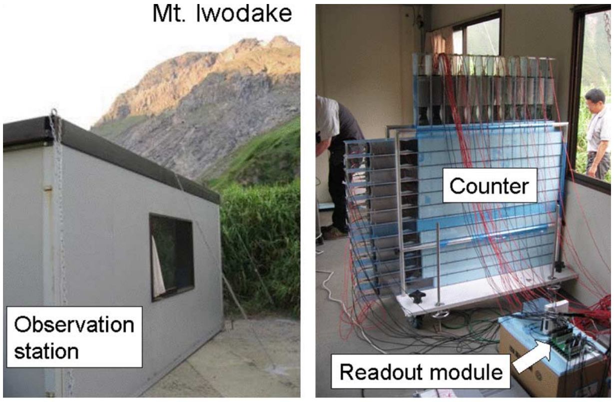

(a) (b)

Fig. 9. Photograph of the observation station and detection system. (a) Observation station with Mt. Iwodake in the background. (b) Detection system installed in the station (other counter not shown).

data to the PC. The histogram is displayed on the web page on the remote PC.

IV. TEST AND RESULTS

The power consumption of the readout module was measured, and a volcano was observed using this readout system.

The measured power consumption of the readout module was about 5 W, including voltage conversion loss from 100VAC to $+5$VDC and -5VDC. The power budget for this module was 10 W. Thus, this measured power consumption was low enough to be supplied by a small solar-powered system.

Beginning in July 2008, this readout system was used to monitor a volcano, Mt. Iwodake (main peak, 703 m in height), on Satsuma-Iwojima island, which is located about 1000 km southwest of Tokyo, Japan. A small prefabricated observation station was constructed near the foot of Mt. Iwodake, about 1.2 km from its peak (Fig. 9(a)). The photograph on the right of Fig. 9(b) shows the counter and readout module of the detection system used in this station. The other counter is not shown. Since commercial power is supplied to this station, a solar-powered system was not used.

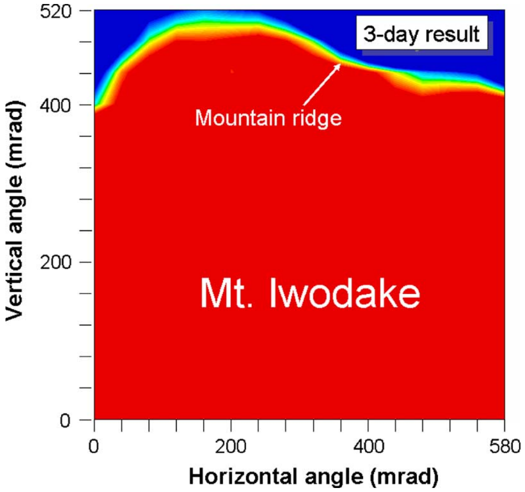

Fig. 10. Radiographic image of Mt. Iwodake. The red and blue areas represent relatively high and low density, respectively.

Fig. 10 shows the first result obtained with this detection system, namely, a radiographic image of Mt. Iwodake. A density profile integrated along the paths of the muons is shown. The red area represents relatively higher density material, with fewer muons detected, while blue area represents relatively lower density material, with more muons detected. This result was obtained from measurements over three days. The analysis process included correcting the efficiencies of the detectors, removing high-frequency components of the image, and normalizing relative to the value of the sky (i.e., the blue area). The line of the mountain ridge is shown clearly. This result shows that the performance of the readout system was sufficient for cosmic-ray muon radiography experiments.

V. SUMMARY

Cosmic-ray muon radiography can be used to probe the internal structure of volcanoes. Because the size and power consumption of a conventional readout system are large, the ability to construct observation stations near volcanoes is limited. To overcome this limitation, we have developed a special readout module for the system. This module generates histograms showing the angular distribution of muons that penetrate a volcano. It is operated by a remote PC using a web browser. The total power consumption of this system is about 55 W. The readout system makes it possible to employ a small solar-powered system and a wireless Local Area Network (LAN). This system was used to monitor a volcano, Mt. Iwodake, in July 2008. Over 3 days, we obtained the first clear, cosmic-ray muon radiography image of this volcano. These findings show that performance of the readout system is sufficient for future observations of other volcanoes by cosmic-ray muon radiography.

REFERENCES

[1] K. Borozdin *et al.*, “Radiographic imaging with cosmic-ray muons,” *Nature*, vol. 422, p. 277, 2003.

[2] L. J. Schultz *et al.*, “Image reconstruction and material Z discrimination via cosmic ray muon radiography,” *Nucl. Instrum. Methods Phys. Res. A*, vol. A519, pp. 687–694, 2004.

[3] L. W. Alvarez *et al.*, “Search for hidden chambers in the pyramids,” *Science*, vol. 167, pp. 832–839, 1970.

[4] K. Nagamine *et al.*, “Method of probing inner-structure of geophysical substance with the horizontal cosmic-ray muons and possible application to volcanic eruption prediction,” *Nucl. Instrum. Methods Phys. Res. A*, vol. A356, pp. 585–595, 1996.

[5] H. Tanaka *et al.*, “Development of the cosmic-ray muon detection system for probing internal-structure of a volcano,” *Hyperf. Interact.*, vol. 138, pp. 521–526, 2001.

[6] H. Tanaka *et al.*, “Development of a two-fold segmented detection system for near horizontally cosmic-ray muons to probe the internal structure of a volcano,” *Nucl. Instrum. Methods Phys. Res. A*, vol. A507, pp. 657–669, 2003.

[7] H. K. M. Tanaka *et al.*, “Radiographic measurements of the internal structure of Mt. West Iwate with near-horizontal cosmic-ray muons and future developments,” *Nucl. Instrum. Methods Phys. Res. A*, vol. A555, pp. 164–172, 2005.

[8] H. K. M. Tanaka *et al.*, “Development of an emulsion imaging system for cosmic-ray muon radiography to explore the internal structure of a volcano, Mt. Asama,” *Nucl. Instrum. Methods Phys. Res. A*, vol. A575, pp. 489–497, 2007.

[9] H. K. M. Tanaka *et al.*, “High resolution imaging in the inhomogeneous crust with cosmic-ray muon radiography: The density structure below the volcanic crater floor of Mt. Asama, Japan,” *Earth Planet. Sci. Lett.*, vol. 263, pp. 104–113, 2007.

[10] H. K. M. Tanaka *et al.*, “Imaging the conduit shape beneath the dome with cosmic-ray muons: The structure beneath Showa-Shinzan lava dome, Japan,” *Geophys. Res. Lett.*, vol. 34, p. L22311, 2007.

[11] Spartan-3AN FPGA Family Data Sheet, DS557, XILINX Inc., 2007.

[12] LAN8700/LAN8700i Data Sheet, Rev. 1.5, SMSC, 2007.

[13] T. Uchida and M. Tanaka, “Development of TCP/IP processing hardware,” in *Proc. IEEE Nuclear Science Symp. Conf. Rec.*, 2006, pp. 1411–1414.

[14] T. Uchida, “Hardware-based TCP processor for gigabit ethernet,” *IEEE Trans. Nucl. Sci.*, vol. 55, no. 3, pp. 1631–1637, Jun. 2008.